PHYSICAL REVIEW B VOLUME 15, NUMBER 1 1 JANUARY 1977

Mössbauer spectroscopy of small gold particles

M. P. A. Viegers and J. M. Trooster
Research Institute for Materials, University of Nijmegen, Toernooiveld, Nijmegen, The Netherlands
(Received 24 May 1976)

The mean-square vibrational amplitude and isomer shift of gold atoms in small particles of gold metal embedded in gelatin were investigated by the Mössbauer effect. Nine samples with average particle diameters of 30–170 Å were examined, three of which (31, 52, and 168 Å) as function of temperature. All samples showed different, but positive, isomer shifts with respect to bulk gold without an apparent correlation with the particle size. At 4.2°K the Mössbauer fraction shows no significant difference with bulk gold, whereas at higher temperatures the Mössbauer fraction decreases more rapidly when the particle size becomes smaller. This temperature dependence is analyzed within the framework of the Debye continuum theory of lattice vibrations, which is a good approximation in case of bulk gold. It is shown that neither the application of a low-frequency cutoff on the phonon spectrum, nor the contribution of surface and edge modes or an independent treatment of bulk and surface atoms gives a satisfactory explanation of the observations, but, that the vibration of the particle as a whole has to be taken into account, which overshadows possible size effects.

I. INTRODUCTION

Recently the properties of small particles have attracted much interest. New phenomena can be expected when the dimensions of the systems become comparable with the characteristic wavelengths of particular physical properties. One of the properties where changes can be expected is the phonon spectrum, and one of the experimental methods, which give information on the phonon frequency distribution is the Mössbauer effect (ME). The intensity of Mössbauer absorption is proportional to

$$f_a(T) = \exp(-4\pi^2\langle x^2\rangle_T/\lambda^2)\,, \tag{1}$$

where $f_a(T)$ is the probability for recoilless absorption (the Mössbauer fraction) at temperature T, $\langle x^2\rangle_T$ the mean-square vibrational amplitude of the absorbing nucleus at temperature T and λ the wavelength of the absorbed radiation.

A sizable number of papers has reported on a study of the phonon spectrum of small particles with the Mössbauer effect, but until now no consistent picture emerges. Marshall and Wilenzick[1] measured the ME of gold particles with an average diameter of 60 and 200 Å. For the 60-Å particles an increase in $f_a(T)$ was found compared with bulk gold, which these authors attributed to a low-frequency cutoff in the phonon spectrum. It is noteworthy that at that time no accurate experimental measurement of $f_a(T)$ in bulk gold had been made. Roth and Hörl[2] measured the ME in 30-Å tungsten particles suspended in frozen organic solvents and found at 78 °K a decrease in f_a compared with the bulk value. Susdalev, Gen, Goldanskii, and Makarov[3] studied tin particles in paraffin with diameters between 1550 and 250 Å and found f_a decreasing with decreasing particle size. Bogomolov and Klushin[4] measured the ME of tin in porous glass with a pore diameter of 70 Å. At temperatures below 100 °K f_a was found to be larger than in bulk tin, but at higher temperatures f_a was smaller than the bulk values at corresponding temperatures. However the values of $f_a(T)$ for bulk tin, given by Bogomolov and Klushin, differ considerably from the very accurate measurements by Hohenemser,[5] which makes the reliability of their data questionable. Akselrod, Pasternak, and Bukshpan[6] measured the temperature dependence of the ME of small (45 Å) tin particles embedded in amorphous SnO. The temperature gradient of $f_a(T)$ was found to be slightly larger than in bulk tin. These authors apparently have not corrected for any saturation effect in the measured absorption intensity presumably because the absorbers used were very thin. It is important to note, however, that an absorber thickness of 1 mg/cm^2 of natural tin at 77 °K already leads to a line shape, which when fitted with a Lorentzian gives an absorption area 7% smaller than without saturation. Neglect of such effects can easily lead to apparent changes in the Debye temperature of the same order of magnitude as found by Akselrod *et al.*[6] Thus the conflicting results of the ME experiments are partly due to unreliable data, but sample preparation may also have effects on the results.[7] Furthermore the role of the medium, supporting the particles, has not been discussed, although considerable differences in Mössbauer fraction were recently found for thin films of tin on different substrates.[8]

In this paper we report a ME study of microcrystals of gold embedded in gelatin. This matrix is well suited to prepare high concentrations of particles with a narrow size distribution. In

Sec. II we give a survey of various models, which can be used to describe the effect of particle size on the phonon spectrum and present the results of a number of calculations. Much effort has been put in the preparation of well-defined samples. These are described in Sec. III together with the measurement techniques. The results are discussed in Sec. IV where we conclude that the matrix supporting the particles has to be taken into account.

II. MÖSSBAUER SPECTROSCOPY AND THE PHONON SPECTRUM

In the harmonic approximation the probability for recoilless absorption is given by Eq. (1). For a monoatomic lattice with a distribution $g(\omega)$ for the phonon frequencies one gets[9]

$$f_a(T)=\exp\left[-\frac{\pi h}{m\lambda^2}\frac{1}{3N}\times\int_0^\infty\frac{g(\omega)}{\omega}\left(\frac{2}{e^{\hbar\omega/kT}-1}+1\right)d\omega\right], \quad (2)$$

where m is the atomic mass, k the Boltzmann constant, h Planck's constant, and N is the number of atoms in the lattice.

In the Debye continuum theory $g(\omega)$ of a cube with edge L is given by[10]

$$g(\omega)=\frac{3L^3}{\pi c^3}\omega^2+\frac{9L^2}{2c^2}\omega+\frac{3L}{8c}. \quad (3)$$

Here c is an average sound velocity. The first term in the right-hand side of Eq. (3) represents the contribution of the bulk phonons, the second term the surface modes, and the last term the edge modes. In bulk the first term on the right-hand side of Eq. (3) dominates and is the only one retained. In this approximation there is an upper limit ω_m for the phonon frequency given by

$$\omega_m^3=3N\pi c^3/L^3, \quad (4)$$

because of the normalization condition

$$\int_0^\infty g(\omega)\,d\omega=3N, \quad (5)$$

where N is the number of atoms in the cube. The maximum phonon frequency is usually expressed in an equivalent temperature, the Debye temperature Θ_D:

$$\Theta_D=\hbar\omega_m/k. \quad (6)$$

Expressing L in Θ_D with help of Eqs. (4) and (6), $g(\omega)$ is given by

$$g(\omega)=(9N\hbar^3/k^3\Theta_D^3)\omega^2 \quad (0<\hbar\omega<k\Theta_D). \quad (7)$$

Using this expression for $g(\omega)$ in Eq. (2) one obtains

$$f_a(T)=\exp\left[-\frac{h^2}{2m\lambda^2}\frac{3}{2k\Theta_D}\times\left(1+\frac{4T^2}{\Theta_D^2}\int_0^{\Theta_D/T}\frac{x\,dx}{e^x-1}\right)\right]. \quad (8)$$

It is customary in Mössbauer spectroscopy to use this expression to calculate an effective Debye temperature Θ_D^M from $f_a(T)$.[11] If $g(\omega)$ deviates from the Debye spectrum, as is generally the case, Θ_D^M is temperature dependent. In that case Θ_D^M also differs from Θ_D^C determined from specific-heat measurements, because both methods measure different moments of $g(\omega)$. For bulk gold, however, the temperature dependence of Θ_D^M as well as the difference between Θ_D^M and Θ_D^C is small.[12] In fact, the temperature dependence of the Mössbauer fraction is very well reproduced by Eq. (8) with $\Theta_D=168\,^\circ$K (see Fig. 7).

In case of small particles an obvious change in the phonon spectrum $g(\omega)$ compared with bulk material will be a low-frequency cutoff ω_L. The longest possible wavelength is of the order of the particle dimension L. If the boundaries of the particle are assumed to be at rest, ω_L is given by

$$\omega_L=\pi c/L. \quad (9)$$

The normalization condition Eq. (5) now becomes

$$\int_{\omega_L}^\infty g(\omega)\,d\omega=3N, \quad (10)$$

resulting in a high-frequency cutoff ω_H given by

$$\omega_H^3=\omega_m^3+\omega_L^3, \quad (11)$$

where ω_m is given by Eq. (4). Expressing ω_H and ω_L in the equivalent temperatures Θ_H and Θ_L the phonon frequency distribution is given by

$$g(\omega)=\frac{9N\hbar^3}{k^3}\left(\frac{1}{\Theta_H^3-\Theta_L^3}\right)\omega^2 \quad (k\Theta_L\leq\hbar\omega\leq k\Theta_H), \quad (12)$$

with $g(\omega)$ given by Eq. (12) the Mössbauer fraction is given by

$$f_a(T)=\exp\left[-\frac{h^2}{2m\lambda^2}\frac{3(\Theta_H^2-\Theta_L^2)}{2k(\Theta_H^3-\Theta_L^3)}\times\left(1+\frac{4T^2}{\Theta_H^2-\Theta_L^2}\int_{\Theta_L/T}^{\Theta_H/T}\frac{x\,dx}{e^x-1}\right)\right]. \quad (13)$$

In general, $\Theta_L\ll\Theta_D$ and $f_a(T)$ is, without loss of accuracy, given by Eq. (8) if we replace the lower limit in the integral by Θ_L/T. Using Eq. (13) $f_a(T)$ was calculated for a number of values of Θ_L. The results are given in Fig. 1. The most con-

spicuous changes are an increase of $f_a(T)$ with increasing Θ_L and a smaller temperature gradient at low temperatures with increasing Θ_L. However, when L is small it is no longer allowed to neglect the contribution of surface and edge modes to $g(\omega)$, as we have done until now, and we show that this has important consequences for $f_a(T)$.

Substituting Eq. (3) into Eq. (2) one obtains

$$f_a(T) = \exp\left(-\frac{h^2}{2m\lambda^2}\frac{1}{3N}[A + B(T) + C(T) + D(T)]\right), \tag{14a}$$

where

$$A = \frac{3\pi}{4k\Theta_L^3}(\Theta_H^2 - \Theta_L^2) + \frac{9\pi}{4k\Theta_L^2}(\Theta_H - \Theta_L) + \frac{9}{4k\Theta_L}\ln\left(\frac{\Theta_H}{\Theta_L}\right), \tag{14b}$$

$$B(T) = \frac{3\pi}{\Theta_L^3}T^2\int_{\Theta_L/T}^{\Theta_H/T}\frac{x\,dx}{e^x - 1}, \tag{14c}$$

$$C(T) = \frac{9\pi}{2\Theta_L^2}T\int_{\Theta_L/T}^{\Theta_H/T}\frac{dx}{e^x - 1}, \tag{14d}$$

$$D(T) = \frac{9}{2\Theta_L}\int_{\Theta_L/T}^{\Theta_H/T}\frac{(1/x)dx}{e^x - 1}, \tag{14e}$$

and the normalization condition gives

$$3N = \int_{\omega_L}^{\omega_H} g(\omega)\,d\omega$$

$$= \frac{\pi}{2\Theta_L^3}(\Theta_H^3 - \Theta_L^3) + \frac{9\pi}{8\Theta_L^2}(\Theta_H^2 - \Theta_L^2) + \frac{9}{4\Theta_L}(\Theta_H - \Theta_L). \tag{14f}$$

In Fig. 2 we give $f_a(T)$ calculated with Eq. (14a) for various values of Θ_L. It is seen that the inclusion of surface and edge modes in the calculation of $f_a(T)$ leads to a decrease of the Mössbauer fraction at low temperatures with increasing Θ_L, contrary to the results given in Fig. 1.

In the foregoing we have used an average sound velocity c and therefore through Eqs. (4) and (9) average cutoff frequencies. However different modes may have different velocities. For instance Love[13] has calculated the maximum wavelength λ_m in a free elastic sphere of diameter d for rotary and radial vibrations and found $d/\lambda_m = 1.8346$ and 0.8160, respectively. For Rayleigh surface modes one finds $C_R = 0.9149C_T$, where C_T is the velocity of bulk transverse waves.[14] Maradudin *et al.*[15] calculated for edge modes $C_E = 0.9013C_T$. Further reductions in the velocities of sound waves can be expected as a result of a weakening of binding forces for the surface atoms. Consequently the low-frequency cutoff should be different for bulk,

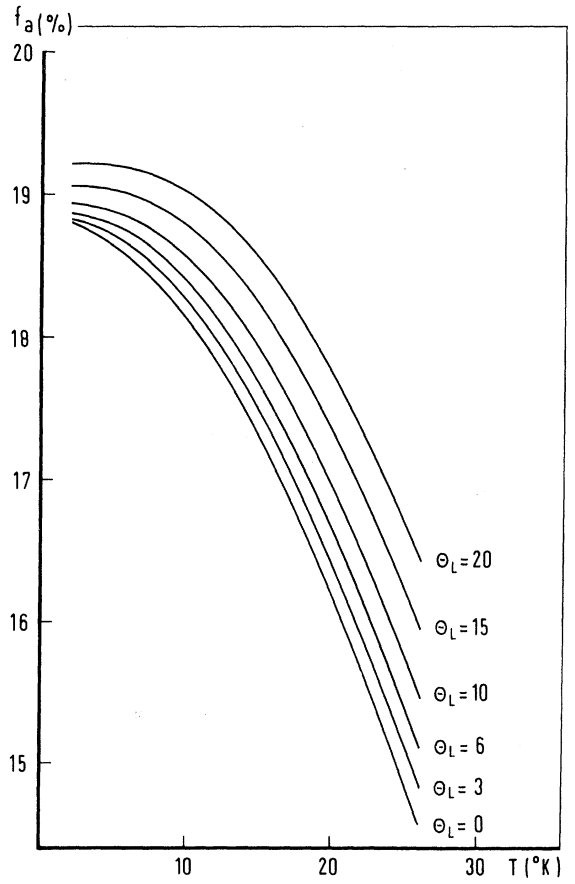

FIG. 1. Temperature dependence of the Mössbauer fraction f_a according to the Debye theory [Eq. (13)] with application of different low-frequency cutoffs on the phonon spectrum, expressed in equivalent temperatures Θ_L. Θ_H was taken to be 170 °K.

surface and edge modes. In comparing calculated and measured values of $f_a(T)$ a further limitation lies in the assumed cubic shape of the particles.

A more serious objection against using the formulas derived above is the fact that we have calculated an average vibrational amplitude which is taken the same for all atoms. In fact we have assumed that every vibrational mode contributes to the amplitude of every atom. Suzdalev *et al.*[5] and later Akselrod *et al.*[6] have circumvented this problem by assigning different Mössbauer fractions f_a^B and f_a^S to bulk and surface atoms, respectively. In that case

$$f_a^{\text{tot}}(T) = \alpha f_a^B(T) + (1 - \alpha)f_a^S(T), \tag{15}$$

where α is the fraction of bulk atoms. For gold this approach is supported by low-energy-electron diffraction measurements of Kostelitz and Domange.[16] These authors find for the surface atoms an effective Debye temperature of Θ_D^S

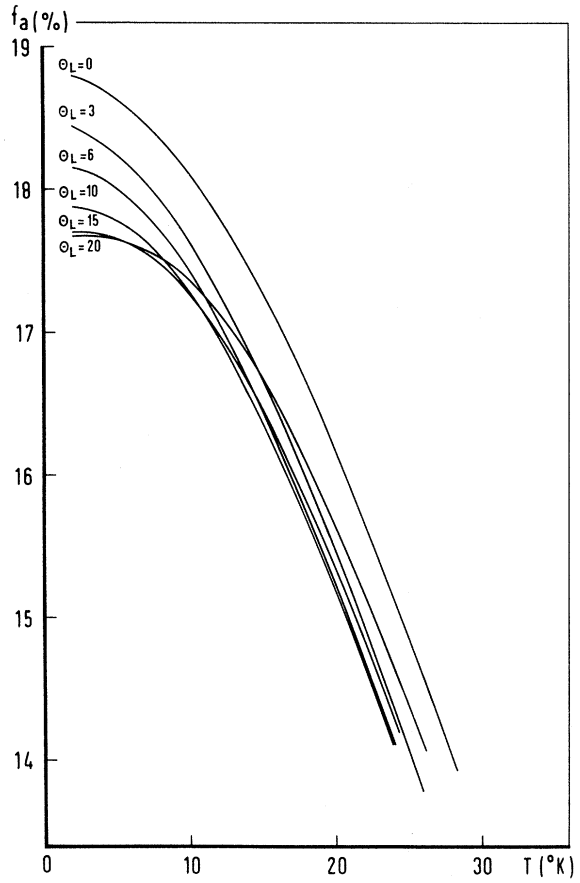

FIG. 2. Temperature dependence of the Mössbauer fraction f_a according to the Debye theory including surface and edge modes [Eq. (14)] for different values of the low-frequency cutoff temperature Θ_L. Θ_L determines also the relative contribution of the surface and edge modes. Θ_H was taken to be 170 °K.

= 83 °K, which means that at $T \ll \Theta_D$ the mean-squared vibrational amplitude of these surface atoms is two times that of bulk atoms.

III. EXPERIMENTAL DETAILS AND RESULTS

A. Sample preparation

The chemistry of hydrosols (colloidal dispersions of solid in water) has been studied extensively.[17] A hydrosol of gold can be prepared by striking an electric arc between gold wires under water or alternatively by reduction of an aquaous solution of auric chloride $AuCl_4^-$. The second method allows a better control of particle size. For this method the competing processes of nucleation and epitaxial growth have been investigated by Turkevich *et al.*[18] These authors found that depending on the nature of the reducing agent and the relative abundance of auric chloride either nucleation or growth is favored.

Coagulation of the gold particles is prevented by a layer of chloride ions on the surface of the particles.[19] The particles then behave like large negative ions and can only exist in very dilute solution. Stabilizers, like gelatin, replace the charged layer on the surface. After such protection of the sol the water can be removed resulting in a high concentration of gold particles. The samples studied in this work have been prepared using as reducing agent either a saturated solution of phosphorus in ether or a sodium citrate solution. To prevent the presence of trace impurities, which cause uncontrolled nucleation, a 1-l glass vessel was cleaned first with aqua regia, then with a detergent, and finally rinsed with distilled water. An 800-ml solution of auric chloride acid containing about 30 mg gold was made neutral with potassium carbonate and under vigorous stirring the reducing agent was added. Dropwise addition of 5 ml of the phosphorus solution over half an hour at room temperature yields an average particle diameter of about 60 Å. Rapid addition favors nucleation above growth and the resulting particles have a diameter of about 30 Å. To remove the excess phosphorus the solution is boiled for 3 h after addition of 0.5-g gelatin. Particles with an average diameter of 150 Å were prepared with 100 ml of a 1% sodium citrate solution as reducing agent. The nuclei formed at room temperature grow to their final size of approximately 150 Å when heated for 2 h at 80 °C. After this the gelatin is added.

In order to remove impurities, especially chloride ions, which may still be bound to the surface of the particles, two techniques were used: (i) dialysis with $\frac{1}{2}$-in. cellulose tubes, and (ii) ion exchange with a mixed bed ion exchange resin. The latter method results in a complete removal of all ionic substances. Both techniques were carried out after the gelatin was added and did not affect the particle size distribution as measured with an electron microscope.

The solutions were dehydrated in a rotating film evaporator and put in Lucite pill boxes. The samples contained approximately 8-at. wt% of gold. After all measurements were carried out the gold content of the samples was determined by atomic absorption. In Table I the preparation and purification treatments and the gold content of the samples are given.

B. Particle-size determination

A probe of each sample was examined with a Philips EM201 electron microscope. Fig. 3 shows an electron micrograph of sample 4 deposited on carbon coated formvar. The size distribution of

TABLE I. List of samples, preparation method, and measured properties.

Sample	Reducing agent	Purification	Gold content (mg/cm^2)	Average diameter (Å)	Effective[a] average diameter (Å)	Coherence length (Å)	Bulk[b] fraction α (%)	Isomer[c] shift (mm/sec)	f_a (4.2 °K) (%)
1	Phosphorus	None	22.0±0.7	52	62	43±4	72	0.042±0.005	17.1±1.0
2	Na citrate	None	26.3±0.8	168	176	80±3	91	0.065±0.006	18.2±1.1
3[d]	Phosphorus	Dialysis plus ion exchange	27.2±0.8 10.5±0.3	31	42	...	55	0.100±0.008	19.3±0.9 20.6±1.1
4	Phosphorus	Dialysis plus ion exchange	6.5±0.2	50	59	...	...	0.073±0.008	19.4±1.0
5	Phosphorus	Dialysis	28.5±0.9	31	42	...	...	0.132±0.008	17.7±0.9
6	Phosphorus	None	11.7±0.4	31	42	...	...	0.131±0.008	18.5±0.9
7	Phosphorus	Ion exchange	20.4±0.6	31	42	...	...	0.061±0.008	20.4±0.9
8	Phosphorus	None	...	55	...	...	...	0.10 ±0.02	...
9	Phosphorus	None	...	55	...	...	...	0.20 ±0.07	...

[a] Weighted with the third power of the diameter.

[b] $1-\alpha$ is the relative number of atoms in surface layer of thickness 2.5 Å averaged over size distribution.

[c] With respect to bulk gold. The values given are based on all measurements carried out at 4.2 °K for each sample. In case of sample 1 the isomer shift of the main line is given.

[d] Two absorbers were made from the same sample.

each sample was determined by measuring the diameter of some 500 particles on similar micrographs. For samples 1, 2, and 3 histograms of the particle size distributions are given in Fig. 4. The measured Mössbauer absorption is essentially a sum of the contributions of all individual atoms, therefore an effective average particle size should be used, obtained by weighting the number of particles of given diameter with the corresponding particle volume. Actual and volume weighted average diameters are given in Table I.

For samples 1 and 2 we have determined the coherence length for Bragg diffraction of Cu ($K\alpha$) x-rays by measuring the width of the Bragg peaks.[20] This method is used often to determine average particle sizes.[7] The results, given in Table I, differ considerably from the particle size measured with the electron microscope. There are two possible explanations for this: a gradient in the lattice constant, as found from molecular dynamic calculations carried out by Burton,[21] or a multiply twinned structure, which has been observed for gold, evaporated on cleaved rocksalt[22] and mica.[23] Multiple twinned structures in gold particles, prepared as described above, were recently observed in our institute by Perenboom.[24]

C. Mössbauer measurements

The parent nucleus for the 77-keV Mössbauer transition of ^{197}Au is ^{197}Pt, which has a half-life of 18 h. For our experiments ^{197}Pt sources were made by neutron irradiation of ^{196}Pt during 24 h in a flux of 2×10^{14} neutrons cm^{-2} sec^{-1}. Two samples of platinum enriched in ^{196}Pt were used: 38-mg Pt, enriched to 55% in ^{196}Pt and 43-mg Pt enriched to 46% in ^{196}Pt. Besides ^{197}Pt other radioactive isotopes are formed in the reactor. The most important of these is ^{199}Au with a half-life of 3.15 days. For the 38-mg source for instance, the activities of ^{197}Pt and ^{199}Au at the end of the irradiation are ~190 and ~15 mCi, respectively.

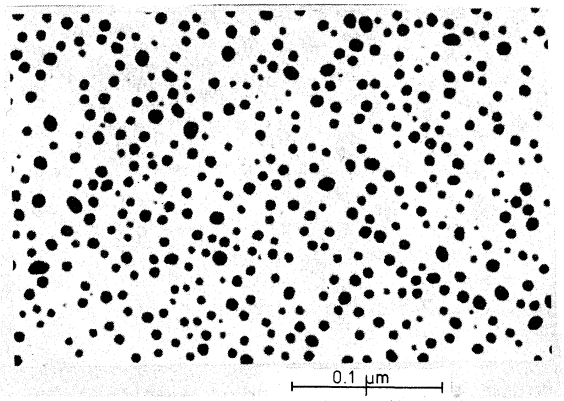

FIG. 3. Electron micrograph of the gold particles in sample 4.

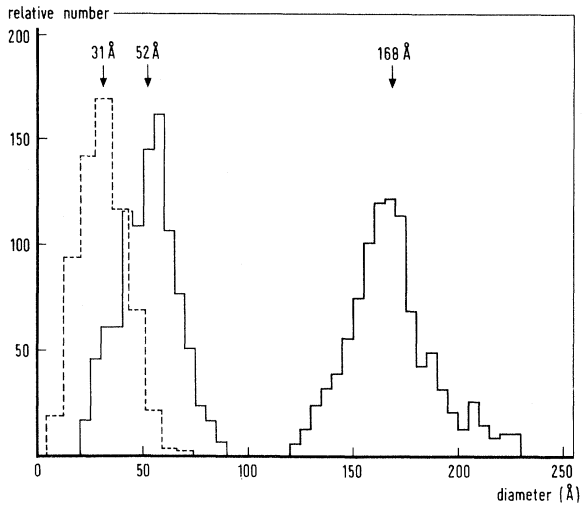

FIG. 4. Size distribution histograms of sample 3 (31 Å), sample 1 (52 Å), and sample 2 (168 Å).

For the Mössbauer experiments the source is mounted together with the absorber in an insert for a liquid-helium cryostat. The source is fixed to a stainless-steel tube connected to an electromechanical drive on top of the cryostat. A mirror on the other side of the drive forms part of a Michelson interferometer used to measure the velocity. The source is moved periodically in a constant acceleration mode: the velocity changes in a triangular way. The absorber is thermally isolated from the helium bath and can be heated to ~100 °K. The temperature is measured with a germanium sensor and the stability was better than 0.05 °K. Velocity and intensity of radiation, transmitted through the absorber, are measured simultaneously and stored in the memory of a multichannel analyzer, running in the time mode. For the detection of the γ rays we used the integrating counting technique described earlier.[25] This method results in short measuring times and enabled us to measure at eight different temperatures with one source.

With the integrating counting technique no energy discrimination is made except for the energy dependent efficiency of the thin (2 mm) NaI(Tl) crystal, used as detector. Because of the different half-lives of ^{197}Pt and ^{199}Au the fraction of ^{197}Au 77-keV γ rays in the measured intensity decreases with time. This time dependence was determined by measuring at regular intervals the spectrum of a gold foil, or, in case of temperature dependent measurements, by measurements

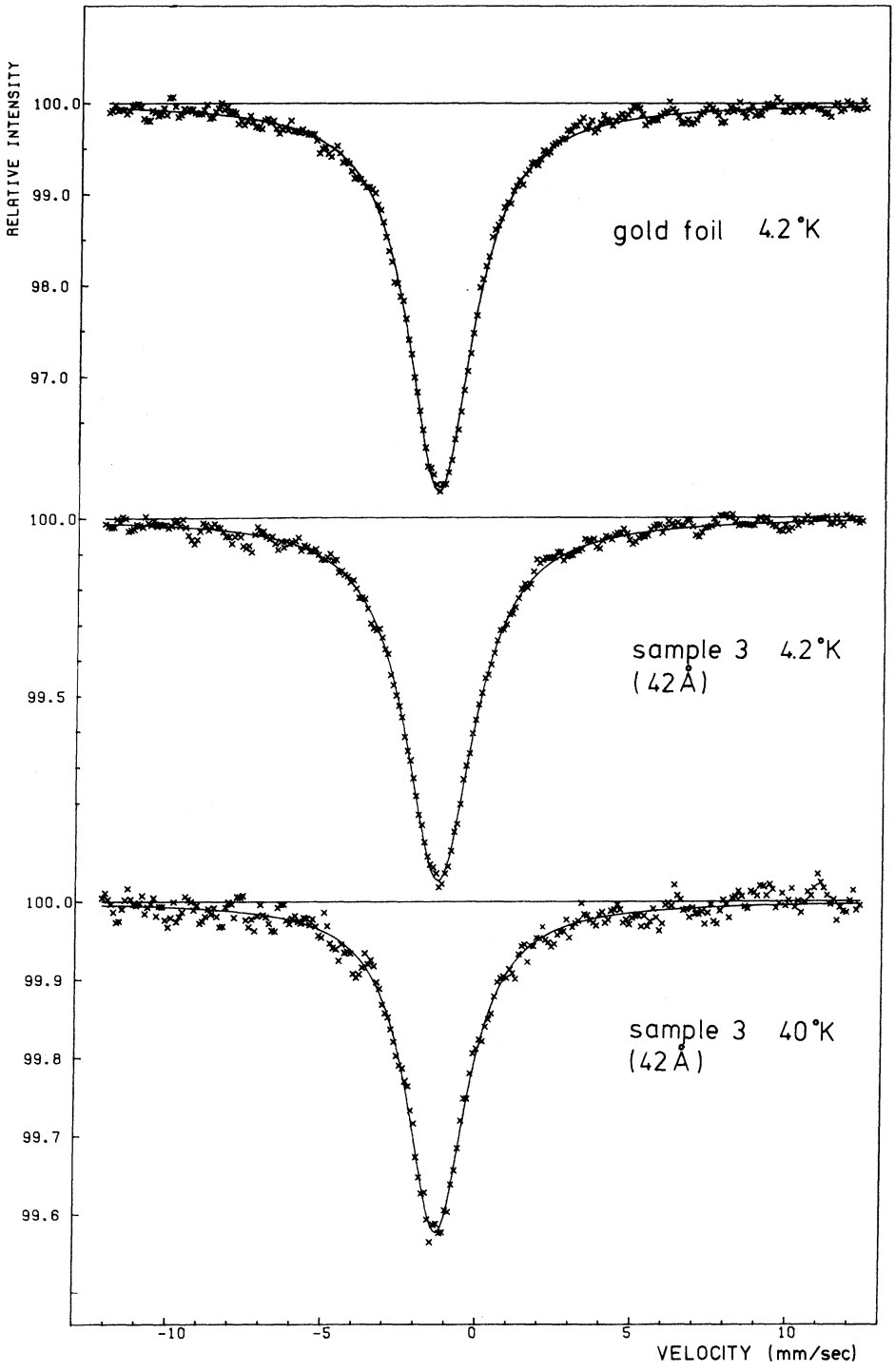

FIG. 5. Mössbauer spectra of a 99-mg/cm^2 gold foil at 4.2 °K and microcrystal sample 3 at 4.2 and 40 °K. The drawn line is a least-squares-fitted Lorentzian.

at 4.2 °K, alternating with the measurements at higher temperatures.

The intensity variation (0.5%) due to the changing distance between source and absorber (solid angle effect) is of the same order of magnitude as the intensity of the Mössbauer absorption. Although this can be taken into account when fitting the spectra, better results are obtained when this baseline curvature is removed by normalizing with a "spectrum" taken without absorber. As explained in Ref. 25 the relative Mössbauer absorption intensity is determined by comparison

with the baseline curvature.

After normalization the spectra are fitted with a Lorentzian. To illustrate the quality of the data we give in Fig. 5 the spectra of sample 3 measured at 4.2 and 40 °K and of a annealed gold foil (99 mg/cm²) measured at 4.2 °K with the same source. The line position of the small particle samples with respect to this gold foil is given in Table I. In the spectra there is no indication of broadening other than caused by saturation effects, except for sample 1 where an asymmetric line shape was observed, see Fig. 6.

The Mössbauer absorption measured is the sum of contributions of individual atoms and the effective Mössbauer absorber thickness T_a is given by[9]

$$T_a = n_0 f_a \sigma , \tag{16}$$

where σ is the resonance cross section and n_0 the number atoms per unit area. The transmission of the absorber is an exponential function of T_a. For a discussion of the relation between T_a and the measured absorption area we refer to the extensive literature on saturation effects.[26] We have taken saturation into account by calculating the theoretical line shape[27] for different values of T_a and fitting these line shapes with a Lorentzian. Thus the relative (Lorentzian) absorption area was obtained as function of T_a. This curve was calibrated with the gold foil of known density. In this procedure we assumed, that the fraction of 77-keV Mössbauer radiation, contributing to the detector current, is independent of the absorber. This means that the differences in nonresonant absorption are neglected. This is justified because the largest contribution to the detector current comes from the 77-keV Mössbauer transition and from Pt and Au x rays in the same energy range. To check this, samples 3 and 4 as well as the gold foil were measured together with a quadrupole split Au(III) compound. The absorption lines of this compound are sufficiently separated from the single gold line to allow direct comparison of the absorption areas. The effective thickness T_a determined in this way agrees within accuracy (±2%) with that obtained by the first method.

From the values of T_a at 4.2 °K, f_a was derived using the known value[12] of σ and the measured n_0. The results are listed in Table I. Errors given are based on the statistical accuracy of the data involved. Systematic errors in f_a may result from slight dehydration of the gelatin, which results in a shrinking of the sample, and from inhomogeneous packing. The latter may be caused by the thready nature of the gelatin.

Temperature-dependent measurements were carried out on samples 1, 2, and 3. For each temperature the absorption area was converted to an effective thickness T_a in the way described above. The temperature dependence of f_a normalized to unity at 4.2 °K is given in Fig. 7. Systematic errors due to inhomogeneous packing and shrinking are thus eliminated. Also given in Fig. 7 is $f_a(T)/f_a(4.2\,°\mathrm{K})$ for bulk gold as measured by Erickson *et al.*[12]

IV. DISCUSSION

A. Phonon spectrum

It appears from the results listed in Table I, that there is no clear correlation between the

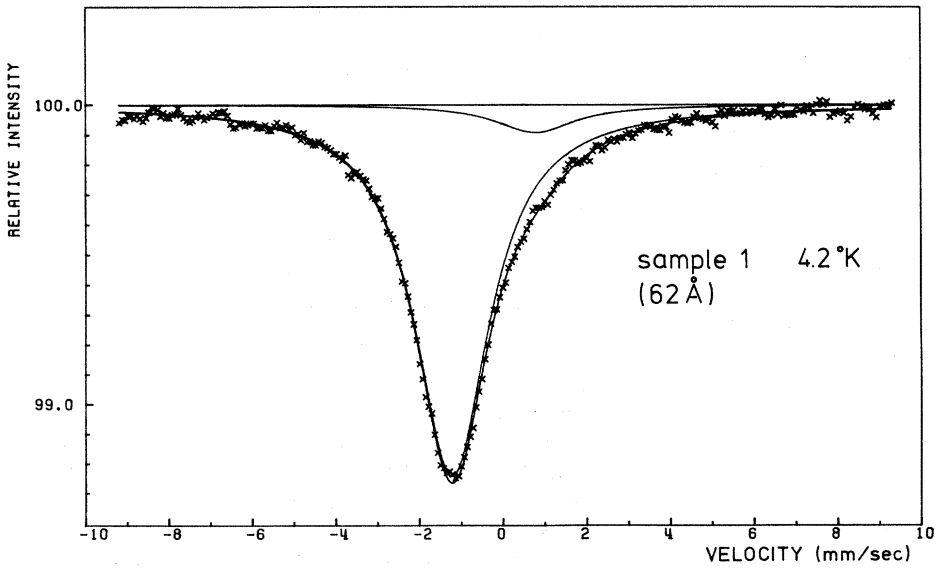

FIG. 6. Asymmetric absorption line shape of sample 1. The spectrum was fitted with two Lorentzians, from which the absorption area was determined.

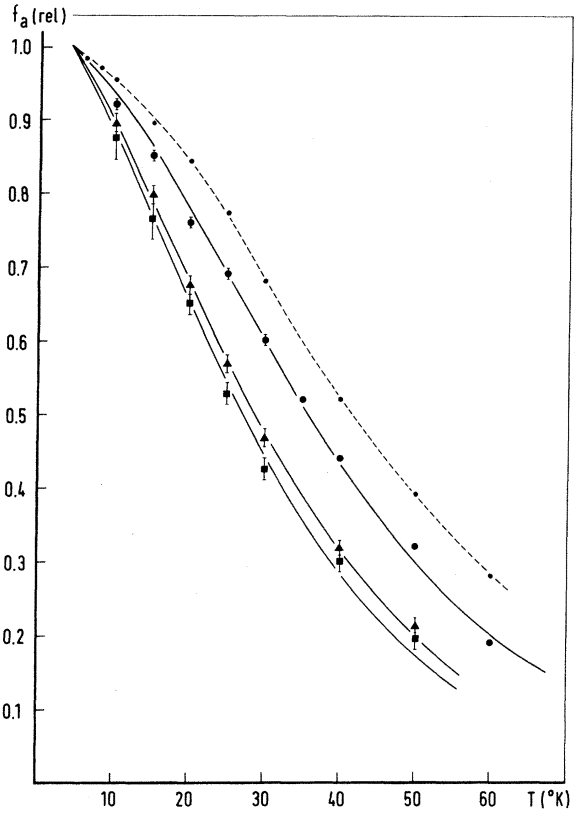

FIG. 7. Observed temperature dependence of the Mössbauer fraction f_a relative to f_a at 4.2 °K. •, bulk gold Ref. 12; ●, sample 2 (176 Å); ▲, sample 1 (62 Å); ■, sample 3 (42 Å). The solid curves are least-squares fits to the experimental points using Eq. (22) (model D). In this model the particles are vibrating as a whole with an Einstein frequency Θ_E, which is the only free parameter in the fit. The vibrations within the particle are described by a Debye spectrum [Eq. (7)], with Θ_D = 168 °K, the value of bulk gold.

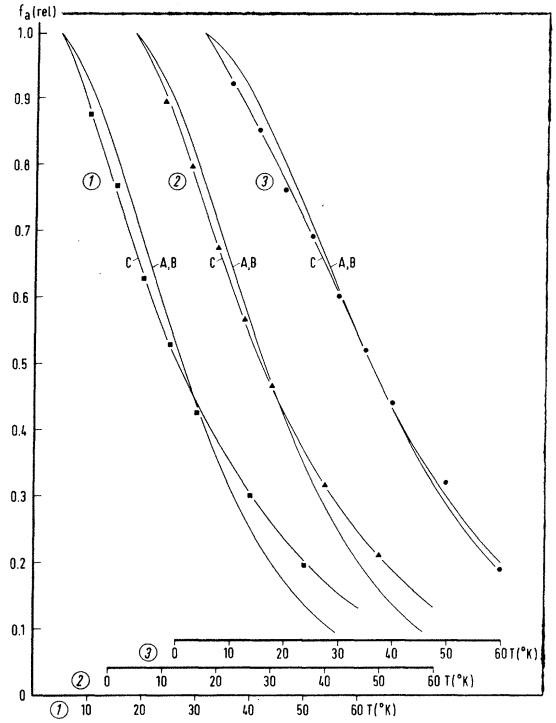

FIG. 8. Least-squares fits to the experimental points. ●, sample 2 (176 Å); ▲, sample 1 (62 Å); ■, sample 3 (42 Å). (A) using the Debye theory [Eq. (8)] with Θ_D as free parameter. (B) using the Debye theory including surface and edge modes [Eq. (14a)] with Θ_L and Θ_H as free parameters. (C) summing the independent contributions of the surface and bulk atoms [Eq. (15)] with Θ_D^{surf}, Θ_D^{bulk}, and α as free parameters.

Mössbauer fraction at 4.2 °K and the average particle diameter. In fact if we average all measured values of f_a we find f_a(4.2 °K) = 18.8%, very close to the value of 18.90% found for bulk gold at 4.2 °K.[12] Thus it can be concluded that at 4.2 °K the Mössbauer fraction of small gold particles in gelatin is not much different from bulk gold. The temperature dependence of f_a on the other hand is clearly correlated with particle size. Any valid explanation of the temperature dependence should result in a value of f_a(4.2 °K) close to the bulk value.

We have tried to fit the measured values of $f_a(T)/f_a$(4.2 °K) with the three models treated in Sec. II. These are the following:

(a) A Debye frequency distribution, Eq. (8). The only free parameter in the fit was Θ_D. The best fits are plotted in Fig. 8 together with the measured points. The corresponding values of Θ_D are listed in Table II together with the Mössbauer fraction at 4.2 °K calculated with the parameters of the best fit. It is clear from Fig. 8 that the single Debye model cannot reproduce the observed temperature dependence. Moreover the calculated Mössbauer fraction at 4.2 °K is too low.

(b) No appreciable improvement is obtained when we use Eq. (14) even though we have now two free parameters Θ_L and Θ_H. See curve B in Fig. 8. In fact the calculated temperature dependence is practically equal to that found with Eq. (8). The parameters corresponding with the curves B in Fig. 8 are given in Table II.

(c) Allowing different vibration amplitudes for bulk and surface atoms by using Eq. (15) with a $f_a^S(T)$ and $f_a^B(T)$ given by Eq. (8) with different Θ_D, excellent fits to the measured $f_a(T)$ are obtained. See Fig. 8, curve C. In the fit three free parameters were used: α, Θ_D^{surf}, and Θ_D^{bulk}. The results are given in Table II. Apart from the fact that α is rather small the calculated value of

TABLE II. Results of least-squares fits to measured temperature dependence of the Mössbauer fraction of samples 1, 2, and 3.

Model A Eq. (8)	Θ_D (°K)	f_a (4.2 °K)$_{calc}$ (%)
Sample 3 (42 Å)	123	9.8
Sample 1 (62 Å)	128	10.7
Sample 2 (176 Å)	148	14.5

Model B Eq. (14a)	Θ_L (°K)	Θ_H (°K)	f_a (4.2 °K)$_{calc}$ (%)
Sample 3 (42 Å)	2.6	129	10.5
Sample 1 (62 Å)	2.6	133	11.4
Sample 2 (176 Å)	2.8	154	15.2

Model C Eq. (15)	α	Θ_D^{bulk} (°K)	Θ_D^{surf} (°K)	f_a (4.2 °K)$_{calc}$ (%)
Sample 3 (42 Å)	0.28	148	78	5.8
Sample 1 (62 Å)	0.37	150	87	7.8
Sample 2 (176 Å)	0.22	153	51	3.7

Model D Eq. (22)	Θ_E (°K)	f_a (4.2 °K)$_{calc}$ (%)
Sample 3 (42 Å)	3.1	16.1
Sample 1 (62 Å)	1.9	16.4
Sample 2 (176 Å)	0.65	17.0

f_a at 4.2 °K is much too low. If Θ_D^{bulk} and Θ_D^{surf} are fixed at 168 and 83 °K, respectively, good fits can still be found, but no appreciable increase in f_a is obtained.

We conclude therefore that none of the models used gives a satisfactory explanation of the measured $f_a(T)$.

In the foregoing discussion we assumed, in line with general practice, that only vibrations within the particle contribute to the vibrational amplitude of the gold atoms. Vibrations of the particle as a whole are assumed to be negligibly small because of the large mass of the particle. On the other hand the opposite approach has been used for molecular crystals.[28] In these crystals molecules are bound by van der Waals forces, that are weak compared with intramolecular forces and the Mössbauer fraction is dominated by the vibrations of the molecular units as a whole in spite of their larger mass. It is illustrative to consider a harmonic oscillator with frequency

$$\omega = (q/m)^{1/2}, \tag{17}$$

where q is the binding force constant and m is the mass of the vibrating particle. The mean-square vibrational amplitude is given by[9]

$$\langle x^2 \rangle = \frac{\hbar}{2m\omega}\left(\frac{2}{e^{\hbar\omega/kT}-1}+1\right). \tag{18}$$

For $T=0$

$$\langle x^2 \rangle = \hbar/2m\omega = \tfrac{1}{2}\hbar(1/qm)^{1/2}, \tag{19}$$

and it is clear that in molecular crystals the effect of the large molecular mass can be compensated by a weaker binding force. For the small particles investigated by us the mass is two orders of magnitude larger than the mass of molecular unit and one may assume that $\langle x^2 \rangle_{T=0}$ is indeed very small. But at the same time ω [Eq. (17)] is reduced and consequently the exponential in Eq. (18) becomes more important at lower temperatures.

In molecular crystals intermolecular vibrations are of the order of 100 °K whereas the mass is typically 3–10 times the mass of the Mössbauer nucleus. Assuming similar binding forces one estimates the vibration frequency of a particle with 10^3–10^4 atoms to be in the order of (1–10) °K. For $kT > 3\hbar\omega$, $\langle x^2 \rangle$ is given by

$$\langle x^2 \rangle = kT/q, \tag{20}$$

and independent of the mass. Thus at very low temperatures the large mass causes such a small vibrational amplitude of the particle that $f_a(T)$ at these temperatures is mainly determined by the vibrations within the particle, but at only slightly higher temperatures the vibration of the particle as a whole results in a considerable decrease of the Mössbauer fraction.

The gold particles investigated by us are bound by van der Waals forces to the gelatin matrix. Because the average distance between the particles is large compared to their diameter, vibrational coupling between the particles can be neglected. The vibration is then best described by a localized mode, so that the Einstein model is applicable. Furthermore we assume that there is no coupling between this Einstein mode and the phonons in the particle. Then

$$\langle x^2 \rangle_{tot} = \langle x^2 \rangle_{part} + \langle x^2 \rangle_{latt}, \tag{21}$$

where $\langle x^2 \rangle_{part}$ is the mean-squared vibrational amplitude of the particle as a whole and consequently

$$f_a^{tot} = f_a^{part} f_a^{latt}. \tag{22}$$

f_a^{part} is given by

$$f_a^{part}(T) = \exp\left[\frac{h^2}{2m\lambda^2}\,\frac{1}{k\Theta_E}\left(\frac{2}{\exp(\Theta_E/T)-1}\right)+1\right] \tag{23}$$

as follows by substituting Eq. (18) into Eq. (1), with $\Theta_E = \hbar\omega/k$ the Einstein temperature.

We applied Eq. (22) to analyze the measured tem-

perature dependence of f_a. For f_a^{latt} Eq. (8) was used with Θ_D held at 168 °K, the value found for bulk gold.[12] The only free parameter in the fit is Θ_E of Eq. (23). For m the mass corresponding with the effective average diameter was used. The values of Θ_E, that gave the best fit are listed in Table II, model D, and the calculated temperature dependence is plotted in Fig. 7. In view of the fact, that only one free parameter is used, the fits are excellent. Moreover the values of Θ_E are of the order of magnitude, derived above, and the absolute Mössbauer fraction calculated with these values agrees reasonably with the measured values (Table I). If Θ_D is also taken as a free parameter, the fits are not significantly improved. Similarly, if for f_a^{latt} Eq. (14a) is used with Θ_L and Θ_H as free parameters, no significant improvement is found, in agreement with the results of fits A and B.

B. Isomer shift

The isomer shift is proportional to the electron density at the nucleus. According to Thomson *et al.*[29] addition of one 6*s* electron results in a shift of + 8 mm/sec. From Table I no simple correlation between isomer shift and particle size can be derived, except that all samples have a shift, positive with respect to bulk gold. As no line broadening is observed, the electron density at the nuclei is the same for surface and inner atoms.

Schroeer[7] has correlated the isomer shift with lattice contraction using two samples of same average size, but giving different isomer shifts. The lattice contraction was determined from the displacement of x-ray Bragg diffraction peaks. This procedure has recently been questioned by Briant and Burton.[30] The shifts observed by us are of the same order of magnitude as those of Schroeer.[7]

V. CONCLUSION

We conclude that to explain the temperature dependence of the Mössbauer fraction of gold microcrystals as well as its value at 4.2 °K it is necessary to take into account the vibration of the particle as a whole. This has implications for the study of the phonon spectrum of small particles by means of the Mössbauer effect, because the vibration of the particle as a whole overshadows possible size effects and if the particles are bound more tightly the nature of the surface will be affected. Motion of the particles does not affect the Debye-Waller factor for neutron or x-ray diffraction, so that these methods are more suitable for the study of the phonon spectrum of small particles. Such methods applied to 107-Å lead particles in porous glass[31] and 234-Å gold particles in an Argon matrix[32] indicate an increase in vibrational amplitude of the atoms.

The importance of the binding of small particles for the Mössbauer effect was earlier pointed out by van Wieringen.[33] In fact van der Giessen, Rensen, and van Wieringen[34] found a large difference in temperature dependence of the Mössbauer fraction of ^{57}Fe in small particles of FeOOH in a gel and dried. Thus it appears that the Mössbauer effect of small particles can be used to study binding to the medium containing the particles rather than the particles themselves.

ACKNOWLEDGMENTS

This investigation was started at the suggestion of Professor P. R. Wyder and supported by the Netherlands Foundation for Chemical Research (SON) with financial aid from the Netherlands Organization for the Advancement of Pure Research (ZWO). A. E. M. Swolfs, J. C. H. van Eijkeren, and M. M. van Deventer assisted with the preparation of the samples and with the measurements.

[1] S. W. Marshall and R. M. Wilenzick, Phys. Rev. Lett. 16, 219 (1966).
[2] S. Roth and E. M. Hörl, Phys. Lett. A 25, 299 (1967).
[3] I. P. Suzdalev, M. Ya. Gen, V. I. Gol'danskii, and E. F. Makarov, Zh. Eksp. Theor. Phys. 51, 118 (1966) [Sov. Phys.-JETP 24, 79 (1967)].
[4] V. N. Bogomolov and N. A. Klushin, Fiz. Tverd. Tela 15, 514 (1973) [Sov. Phys.-Solid State 15, 357 (1973)].
[5] C. Hohenemser, Phys. Rev. A 139, 185 (1965).
[6] S. Akselrod, M. Pasternak, and S. Bukshpan, Phys. Rev. B 11, 1040 (1975).
[7] D. Schroeer, R. F. Marzke, D. J. Erickson, S. W. Marshall, and R. M. Wilenzick, Phys. Rev. B 2, 4414 (1970).
[8] V. N. Epikhin and I. N. Nikolaev', Fiz. Tverd. Tela 16, 3120 (1974) [Sov. Phys.-Solid State 16, 2017 (1975)].
[9] H. Wegener, *Der Mössbauer Effect und Seine Anwendung in Physik und Chemie* (Bibliographisches Institut AG, Mannheim, 1965).
[10] E. W. Montroll, J. Chem. Phys. 18, 183 (1950).
[11] R. H. Nussbaum, *Interpretation and Applications of Mössbauer Fraction Experiments*, *Mössbauer Effect Methodology* (Plenum, New York, 1966), Vol. 2.
[12] D. J. Erickson, L. D. Roberts, J. W. Burton, and J. O. Thomson, Phys. Rev. B 3, 2180 (1971).
[13] A. E. H. Love, *A Treatise on the Mathematical Theory of Elasticity* (Dover, New York, 1944), p. 278.
[14] See Ref. 13, p. 308.

[15]A. A. Maradudin, R. F. Wallis, D. L. Mills, and R. L. Ballard, Phys. Rev. B 6, 1106 (1972).
[16]M. Kostelitz and J. L. Domange, Solid State Commun. 13, 241 (1973).
[17]*Colloid Science*, edited by H. R. Kruyt (Elsevier, Amsterdam, 1952).
[18]J. Turkevich, P. C. Stevenson, and J. Hillier, Discuss. Faraday Soc. 11, 55 (1951).
[19]W. Pauli, Trans. Faraday Soc. 31, 11 (1935).
[20]H. P. Klug and L. E. Alexander, *X-Ray Diffraction Procedures* (Wiley, New York, 1959), Chap. 9.
[21]J. J. Burton, J. Chem. Phys. 52, 345 (1970).
[22]S. Ogawa and S. Ino, J. Cryst. Growth 13/14, 48 (1972).
[23]J. G. Allpress and J. V. Sanders, Surf. Sci. 7, 1 (1967).
[24]J. A. A. J. Perenboom (private communication).
[25]M. P. A. Viegers and J. M. Trooster, Nucl. Instrum. Methods 118, 257 (1974).
[26]S. Margulies and J. R. Ehrman, Nucl. Instrum. Methods 12, 131 (1961); D. A. Shirley, M. Kaplan, and P. Axel, Phys. Rev. 123, 816 (1961); G. A. Bykov and Pham Zuy Hien, Zh. Eksp. Teor. Fiz. 43, 909 (1962) [Sov. Phys.-JETP, 16, 646 (1963)]; G. Lang, Nucl. Instrum. Methods 24, 425 (1963); J. M. Williams and J. S. Brooks, *ibid.* 128, 363 (1975).
[27]T. E. Cranshaw, J. Phys. E 7, 122 (1974).
[28]*Chemical Applications of Mössbauer Spectroscopy*, edited by V. I. Gol'danskii and R.H. Herber (Academic, New York, 1968), Chap. 1.
[29]J. O. Thomson, F. E. Obenshain, P. G. Huray, J. C. Love, and J. Burton, Phys. Rev. B 11, 1835 (1975).
[30]C. L. Briant and J. J. Burton, Surf. Sci. 51, 345 (1975).
[31]V. Novotny, T. M. Holden, and G. Dolling, Can. J. Phys. 52, 748 (1974).
[32]Yu. I. Petrov and V. A. Kotel'inkov, Fiz. Tverd. Tela, 13, 313 (1971) [Sov. Phys.-Solid State, 13, 255 (1971)].
[33]J. S. van Wieringen, Phys. Lett. A 26, 370 (1968).
[34]A. A. van der Giessen, J. G. Rensen, and J. S. van Wieringen, J. Inorg. Nucl. Chem. 30, 1739 (1968).

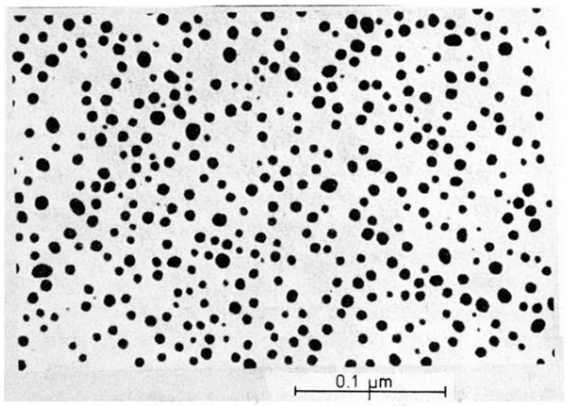

FIG. 3. Electron micrograph of the gold particles in sample 4.